Gold Photochemistry

DOI: 10.1002/ange.201305487

Photoinduced Gold(I)–Gold(I) Chemical Bonding in Dicyanoaurate Oligomers**

Ganglong Cui, Xiao-Yan Cao, Wei-Hai Fang, Michael Dolg,* and Walter Thiel**

Gold chemistry is currently one of the most rapidly growing fields of chemistry. In particular, Au^{I} and Au^{III} complexes have attracted much recent attention in materials science, medicine, heterogeneous, and homogeneous catalysis.[1,2] A characteristic feature of Au is the strong relativistic effects,[3,4] that is, a dominating direct and a weaker indirect stabilization and contraction of the 6s shell, as well as an indirect destabilization and expansion of the 5d shell. The 6s and 5d shells of Au are thus both energetically and spatially closer than in a nonrelativistic approximation, or than the corresponding valence shells of the lighter homologues Cu and Ag. Therefore, relativistic effects have a strong impact on Au chemistry.[5] They also enhance significantly the strong noncovalent Au–Au interaction termed "aurophilicity",[6] which plays an important role in the self-assembly of Au complexes in the ground state, and may also contribute to Au–Au chemical bonding in excited states.[7–11] Au^{I} complexes show great potential in optoelectronic materials such as light-emitting diodes (LEDs), and hence the past decade has also witnessed a growing interest in excited-state properties of polynuclear Au complexes.[12–23]

The prototypical dicyanoaurate $[Au(CN)_2^-]$ has remarkable spectroscopic and excited-state properties in solution.[24–26] Upon progressively increasing the solute concentration, new bands appear continually in the absorption and emission spectra that have been assigned to dicyanoaurate oligomers.[24,25] The positions and intensities of these bands vary with experimental conditions (concentration, temperature, and solvent), thus suggesting the involvement of different oligomers. The character of the emitting states, which is essential for understanding and designing LEDs, is not yet firmly established. There is experimental evidence for a substantial tightening of the Au–Au bond in dicyanoaurate oligomers upon photoexcitation.[24,25] To shed light on this unusual excited-state bonding phenomenon, Iwamura et al. recently employed femtosecond and picosecond time-resolved absorption and emission spectroscopy to explore the excited-state dynamics of the dicyanoaurate trimer $[Au(CN)_2^-]_3$ in aqueous solution.[26] A distinct oscillation of the transient absorption was observed on the femtosecond time scale that was attributed to coherent Au–Au stretching motions associated with excited-state Au–Au bond shortening. However, the origin of this photoinduced enhancement of Au–Au bonding in $[Au(CN)_2^-]_n$ remains elusive.

Previous theoretical studies[25,26] have addressed the ground and lowest triplet states of the dicyanoaurate dimer $[Au(CN)_2^-]_2$ and trimer $[Au(CN)_2^-]_3$, but not the corresponding singlet excited states. The structures and properties of the latter are obviously important for assigning fluorescence bands and understanding excited-state relaxation dynamics, because they are first populated in the Franck–Condon (FC) region and thus provide the starting point for the following photophysical and photochemical processes. To our knowledge, the dicyanoaurate tetramers and pentamers have not yet been theoretically investigated, in spite of the fact that their geometric and electronic structures are relevant for spectroscopic assignments. Here we report electronic structure calculations at the DFT, TD-DFT, RI-CC2, and MS-CASPT2 levels for all these oligomers and for all relevant states. The computational methods, their validation, and detailed numerical results are presented in the Supporting Information.

In the staggered ground-state dimer structure, the two monomers associate because of the noncovalent aurophilic interaction.[8,11] They adopt a perpendicular arrangement. The Au···Au distance in this dimer is computed to be 3.014 Å at the MP2/PCM level (Figure 1), which is close to the previous gas-phase MP2 value of 2.960 Å.[25] All attempts to fully optimize the structure of the eclipsed dimer ended up at the staggered dimer, indicating that the eclipsed conformer is not stable in the ground state. The computed potential energy profile (Figure SI-1) shows that the eclipsed conformer lies only 4.0 kcal mol^{-1} above the staggered one in aqueous solution, implying that the former can become a minimum in rigid surroundings[11] through stabilizing steric interactions.

Contrary to the situation in the S_0 state, stable minima were found both for the staggered and eclipsed dimers in the T_1 and S_1 states. The Au–Au bond length in the T_1 [S_1] state is 2.700 [2.720] Å for the former and 2.708 [2.734] Å for the latter. In both states, the staggered dimer exhibits an almost perpendicular arrangement with a C-Au-Au-C dihedral angle of about 90°; while the eclipsed dimer has a slightly twisted

[*] Dr. G. Cui, Prof. Dr. W.-H. Fang
Chemistry College, Beijing Normal University
Beijing 100875 (China)
E-mail: fangwh@bnu.edu.cn
Dr. G. Cui, Prof. Dr. W. Thiel
Max-Planck-Institut für Kohlenforschung
Kaiser-Wilhelm-Platz 1, 45470 Mülheim an der Ruhr (Germany)
E-mail: thiel@kofo.mpg.de
Dr. X.-Y. Cao, Prof. Dr. M. Dolg
Institut für Theoretische Chemie, Universität zu Köln
Greinstr. 4, 50939 Köln (Germany)
E-mail: m.dolg@uni-koeln.de

[**] W.F. thanks the Major State Basic Research Development Programs (grant number 2011CB808503) and the NSFC (grant number 21033002). G.C. thanks the Alexander-von-Humboldt foundation.

Supporting information for this article is available on the WWW under http://dx.doi.org/10.1002/anie.201305487.

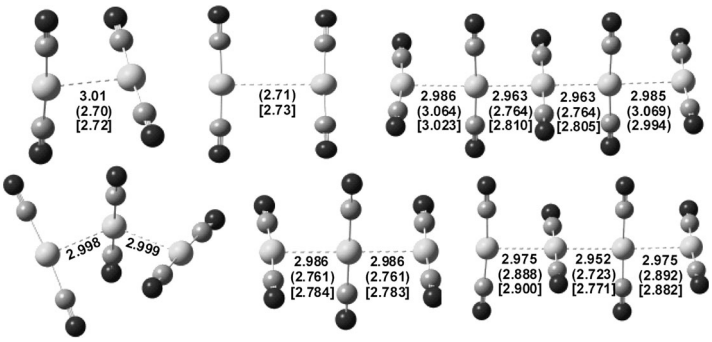

Figure 1. Structures of $[Au(CN)_2^-]_n$ ($n=2$–5) with Au–Au bond lengths (Å) in the S_0, (T_1), and [S_1] states computed at the MP2/PCM (CAM-B3LYP/PCM), and [TD-CAM-B3LYP/PCM] levels.

structure with a dihedral angle of about 30° because of the repulsive interactions between the nearby cyano groups.

In the following molecular orbital (MO) analysis of the T_1 and S_1 states, the Au–Au bond defines the *x* axis (see Figure SI-2), and the MOs are characterized with regard to this axis (σ vs. π). In previous experimental work,[9,25,26] the T_1 state of the staggered dimer was considered to be of σ*σ type, corresponding to the HOMO→LUMO transition from the highest occupied to the lowest unoccupied MO. The HOMO is an antibonding σ* MO mainly composed of Au 5d with considerable 6s contribution, while the LUMO is a bonding σ MO composed of Au $6p_x$ orbitals. The MO analysis at the TD-DFT and MS-CASPT2 levels demonstrates that this σ*→σ ($6p_x$) picture remains valid for the S_1 staggered excimer (see the top panel of Figure 2).

In the eclipsed dimer, we find another excited-state bonding pattern of σ*→π ($6p_z$) type, both in the triplet and singlet manifold (see the bottom panel of Figure 2), with a transition from the σ* HOMO to an unoccupied π MO composed of the Au $6p_z$ orbitals. In the FC region, the ^{1}σ*σ ($6p_x$) state (S_2) is higher in energy than the dark ^{1}σ*π ($6p_z$) state (S_1). The S_2–S_1 energy gap at the S_1 minimum is computed to be 10.2 and 12.0 kcal mol^{-1} at the TDDFT/PCM and MS-CASPT2/PCM levels, respectively. Thus, there is little doubt that this dark state will play an important role in the photophysical processes of the dicyanoaurate dimer. Similar electronic structure features may be expected for pseudo-planar gold complexes with a similar Au–Au skeleton.[11]

For the trimer, Iwamura et al.[26] optimized the staggered structure in the T_1 state at the TD-PBE0/PCM level, without addressing the S_0 and S_1 structures. We have optimized the relevant stationary points in all three states. In the S_0 state, we obtain two staggered minima at the MP2/PCM level (Figure 1), a bent form with an Au–Au–Au angle of 125° and a linear one with an angle of 180°, both with Au–Au bond lengths of around 3.00 Å. At the MP2/PCM level, there is an energy gap of 0.7 kcal mol^{-1} between these two minima so that each of them should contribute to the photophysics of the trimer. In the S_1 and T_1 states, the only minimum is the staggered linear structure, with rather short Au–Au bonds of 2.76 and 2.78 Å, respectively. Closer examination of the MOs indicates a dominant σ*σ ($6p_x$) bonding pattern in these excited states of the trimer.

Born–Oppenheimer molecular dynamics (BOMD) simulations in aqueous solution at the MP2/PCM level show that the bent-to-linear relaxation process of the staggered trimer in the T_1 state is ultrafast (completed within ca. 1 ps, Figure 3). Starting from the FC region, one Au–Au bond length rapidly decreases from initially 3.0 Å to 2.6 Å within 200 fs; then, after two vibrational periods of the Au–Au stretching mode (ca. 650 fs), the system starts Au–Au oscillations around the T_1 equilibrium value of 2.76 Å. The other Au–Au bond exhibits a similar relaxation behavior but fluctuates around its equilibrium value only after four periods (ca. 1300 fs). The Au–Au–Au angle quickly increases to 180° within the first 500 fs and starts regular oscillations after about 2000 fs. In the present dynamics runs, the bent T_1 state thus approaches the linear equilibrium form on the femto-

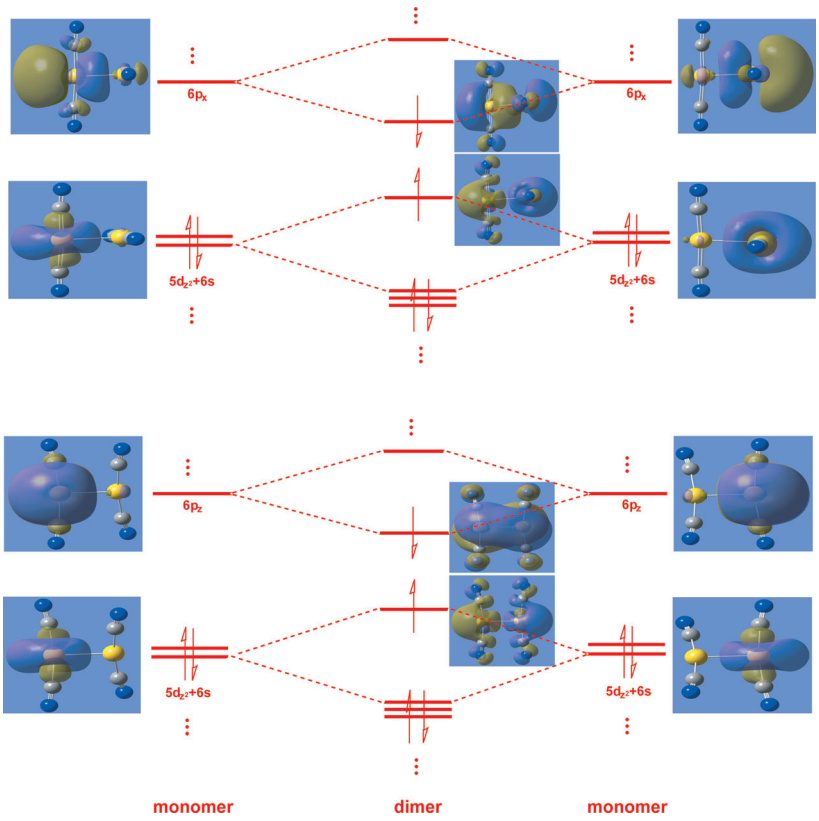

Figure 2. MO plots illustrating two Au–Au bonding patterns for the S_1 dimer. Upper panel: σ*σ transition from the σ* HOMO to the $6p_x$-based σ LUMO; lower panel: σ*π transition from the σ* HOMO to the unoccupied $6p_z$-based π MO. The main MO coefficients from NBO analysis are given in parentheses.

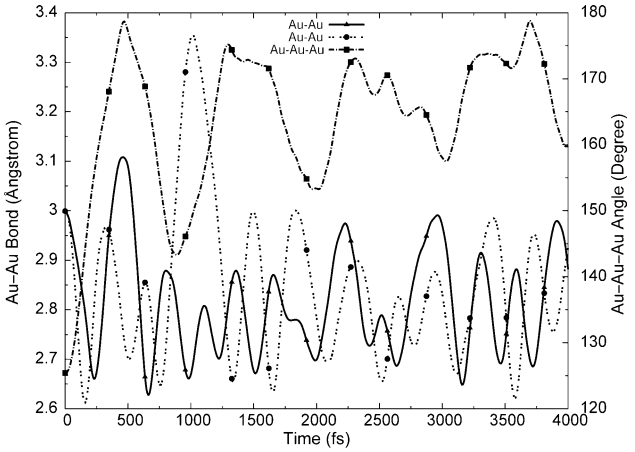

Figure 3. Time-dependent evolution of the Au–Au bond lengths (Å, left axis) and the Au–Au–Au angle (degree, right axis) in a 4 ps BOMD simulation in solution starting from the T_1 FC region of the staggered bent trimer.

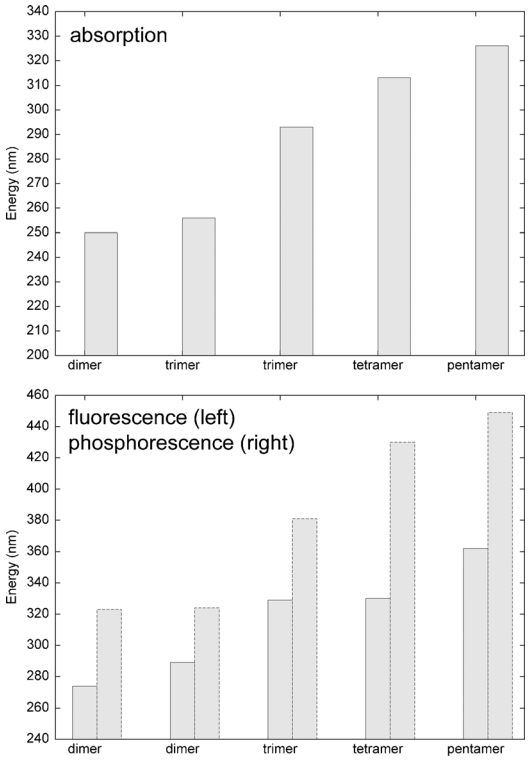

Figure 4. MS-CASPT2/PCM computed absorption (top panel) and emission (fluorescence and phosphorescence, bottom panel) wavelengths. Note that both absorption and emission spectra exhibit a remarkable red shift.

second time scale; the bent-to-linear relaxation time in the BOMD simulations is in good agreement with the experimental estimate of 2.1 ps.[26]

In the excited states of the dicyanoaurate tetramer and pentamer, the central Au–Au bonds are significantly shorter than those on the two sides (see Figure 1), reflecting a spatially local excited-state Au–Au bond tightening (see the Supporting Information for an analysis of the electronic structure of the corresponding excimers).

The absorption spectrum of dicyanoaurate in solution shows an increasing red shift with increasing solute concentration.[24] In dilute solution (1.0×10^{-2} M), the absorption spectrum has a low-energy band in the 250–270 nm region. On the basis of our MS-CASPT2/PCM computations (Figure 4 and Table SI-3), this band corresponds to the bright $S_0\rightarrow S_1$ electronic excitation (245 nm) of the staggered dimer structure; however, there may also be a contribution of the staggered bent trimer structure (256 nm). If the solute concentration increases to 0.3 M, a new absorption band appears around 310 nm. It is commonly accepted that this band arises from the trimer. Our current theoretical work supports this viewpoint but provides further insight. Since the $S_0\rightarrow S_1$ electronic transition of the staggered bent trimer is computed at 256 nm, the new band should be associated with the staggered linear trimer (293 nm), and there could also be a contribution from the staggered linear tetramer (313 nm). The computed absorption maximum (326 nm) of the staggered linear pentamer seems to match with the experimental absorption band (330–350 nm) that is observed at a solute concentration of 0.50–0.76 M.[24]

The emission spectra of the dicyanoaurate oligomers are more complicated due to the mixing of fluorescence and phosphorescence. Patterson and co-workers observed five emission bands (I, II, III, IV, and V) under different experimental conditions of concentration, excitation wavelength, solvent, and temperature (see their Figure 9 and Table 4).[25] Band I (275–285 nm) was assumed to arise from dimer emission, but the nature of the emitting state was unclear. Our MS-CASPT2/PCM results suggest that this band corresponds to the fluorescence emission from both dimer structures, staggered at 274 nm and eclipsed at 289 nm. Experimentally, this emission was monitored using 250 nm excitation, which coincides with the computed absorption maximum of the staggered dimer structure (250 nm, Table SI-3). Band II at 320–350 nm was assigned to the trimer.[25] According to our calculations, band II should have important contributions from the fluorescence of the staggered linear trimer (329 nm) and tetramer (330 nm), and possibly also from phosphorescence of the two dimer structures (staggered at 323 nm and eclipsed at 324 nm). Concerning the experimentally unassigned bands III–V, our calculations attribute band III at 380–390 nm to the phosphorescence emission of the trimer (381 nm); band IV at 420–440 nm lies around the computed phosphorescence emission of the staggered linear tetramer (430 nm), and band V at 455–470 nm may be ascribed to the phosphorescence of the staggered linear pentamer (449 nm).

The excited-state relaxation dynamics of the dimer depends on its conformation. In the staggered structure, the S_1 state is of $\sigma^*\rightarrow\sigma$ ($6p_x$) character and thus spectroscopically bright (oscillator strength: 0.96 at TD-CAM-B3LYP level). It lies far below the higher excited singlet states, which are not accessible upon low-energy photoexcitation. Hence the photophysical processes in the staggered dimer can be described with a three-state model. The staggered S_1 state is first populated in the FC region upon photoexcitation, and

then the Au–Au metal bond is immediately formed during the relaxation process to the staggered S_1 minimum. As a consequence of the strong spin–orbit coupling (SOC) in gold complexes (the 5d shell of Au exhibits the highest SOC constant, 5104 cm^{-1}, among all elements in the first three transition-metal rows),[15,27] an efficient intersystem crossing takes place to the T_1 state, where radiative and radiationless processes as well as reactions can occur (see the top panel of Figure 5).

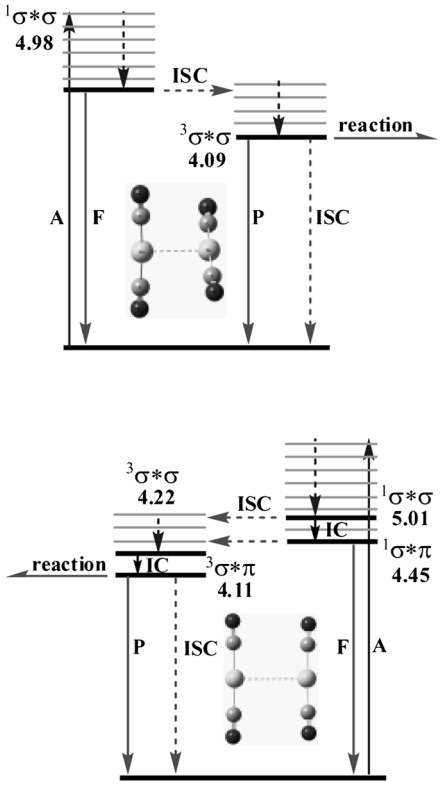

Figure 5. Photophysical mechanisms in the $[Au(CN)_2^-]_2$ dimer. Top: staggered dimer. The S_1 state is a bright $\sigma^*\sigma$ ($6p_x$) state lying far below the higher singlet states. Bottom: eclipsed dimer. The bright $\sigma^*\sigma$ ($6p_x$) S_2 state and the dark $\sigma^*\pi$ ($6p_z$) S_1 state are close to each other. Energies in eV. ISC = intersystem crossing, IC = internal conversion, A = absorption, P = phosphorescence, and F = fluorescence.

The eclipsed form of the dimer is not a minimum in the S_0 state, but it is only about 4 kcal mol^{-1} higher in energy than the staggered form at the MP2/PCM level (Figure SI-1). In rigid surroundings, such as in crystals and certain aggregates, the eclipsed structure is known to be stable.[7] Therefore, we also need to consider its photodynamics to understand the optical properties of dicyanoaurate oligomers in the condensed phase. The excited-state relaxation dynamics of the eclipsed dimer is rather complicated, because the S_2 ($^1\sigma^*\sigma$ ($6p_x$)) and S_1 ($^1\sigma^*\pi$ ($6p_z$)) states as well as their triplet counterparts (T_2 and T_1) are structurally and energetically close to each other. The S_2 state is a bright excited state while S_1 is a dark state with relatively low energy, which is therefore expected to be involved in excited-state relaxation processes. Thus, a five-state model is needed to describe the photophysics (see the bottom panel of Figure 5).

In this model, the bright S_2 state is initially populated in the FC region, from which internal conversion to S_1 (referred to as IC1) and intersystem crossing to T_2 (ISC2) or T_1 (ISC1) can readily occur. In view of the strong SOC interaction in gold complexes,[15] ISC1 and ISC2 should take place with high efficiency. As pointed out before, the S_2 and T_2 states originate from the same $\sigma^*\rightarrow\sigma$ ($6p_x$) electronic transition. In ISC2, there is thus only a spin flip, and hence the total angular momentum is not conserved in this process. In ISC1, by contrast, the spin angular momentum change can be matched by the orbital angular momentum change associated with the $6p_x\rightarrow6p_z$ transition during $S_2\rightarrow T_1$ conversion. The total angular momentum (spin plus orbital components) can thus be conserved in ISC2 so that this process should be faster than ISC1. For analogous reasons, intersystem crossing from the S_1 state will proceed more easily to T_2 than to T_1. Qualitatively, among the four possible nonadiabatic processes from S_2 to T_1, the direct ISC2 pathway should be the most favorable one for the eclipsed dimer. This excited-state relaxation mechanism is expected to play an important role especially in rigid surroundings that stabilize the eclipsed form.[11]

On the basis of the experimental findings for the dicyanoaurate trimer in aqueous solution, Iwamura et al. proposed the following scenario for the excited-state dynamics.[26] The bright S_1 ($^1\sigma^*\sigma$) state is populated in the FC region (staggered bent) and then relaxes rapidly to the S_1 minimum, concomitant with a shortening of the Au–Au bond but still remaining in the staggered bent form, followed by an efficient intersystem crossing to the T_1 ($^3\sigma^*\sigma$) state after about 0.5 ps. In the T_1 state, the bent-to-linear structural transformation occurs within about 2 ps (consistent with our BOMD simulation, see Figure 4 and the related discussion).[26] The resulting staggered linear trimer associates another monomer within about 2 ns, thus forming a tetramer in the T_1 state. In this scenario, phosphorescence can be emitted from the staggered bent and linear trimer as well as from the tetramer, while fluorescence originates from the originally formed staggered bent trimer structure in the S_1 state.[26]

Our present computational results for the trimer are overall in line with this proposed mechanism but suggest some modifications. First, the staggered bent structure is not a minimum in the S_1 or T_1 state of the trimer: after the S_1 state is populated in the FC region, it will rapidly relax to the S_1 minimum, a staggered linear structure, with formation of the Au–Au bond. Second, the $S_1\rightarrow T_1$ intersystem crossing should take place at the staggered linear structure after this fast relaxation process. Third, since the staggered bent and linear structures are almost degenerate minima in the S_0 state (with an energy gap of about 1 kcal mol^{-1} at the MP2/PCM level), one should consider excited-state relaxation processes starting from both structures on an equal footing.

To summarize, we have used high-level ab initio calculations to assign the band maxima of the absorption and emission spectra and to study the excited-state properties of dicyanoaurate oligomers $[Au(CN)_2^-]_n$ ($n = 2$–5) in aqueous solution. The five emission bands observed experimentally were partly reinterpreted and the emitting states were

identified. The lowest excited states were characterized in terms of the leading $\sigma^*\sigma$ ($6p_x$) and $\sigma^*\pi$ ($6p_z$) transitions: the former generally strengthens Au–Au bonding in the lowest bright excited state of the staggered conformers, while the latter helps stabilize the lowest dark state of the eclipsed dimer structure. Furthermore, we explored the photoinduced processes in the dicyanoaurate oligomers. We found that the bright S_1 ($^1\sigma^*\sigma$ ($6p_x$)) state and the corresponding T_1 state are much lower in energy than the higher excited states in the staggered structures ($n = 2$–5), and hence a three-state model should be adequate to describe their excited-state relaxation dynamics. By contrast, a five-state model needs to be used for the almost planar (eclipsed) structures, because the bright S_2 ($^1\sigma^*\sigma$ ($6p_x$)) and the dark S_1 ($^1\sigma^*\pi$ ($6p_z$)) states as well as their triplet counterparts are structurally and energetically close to each other. These insights into excited-state electronic structure should also be relevant for other gold complexes with a similar Au–Au scaffold, and thus facilitate the qualitative understanding of their excited-state properties as well as the design of improved photoluminescent gold complexes.

Received: June 26, 2013
Published online: August 12, 2013

Keywords: Au–Au bonds · aurophilicity · electronic structure · excited states · photochemistry

[1] A. Hashmi, *Chem. Rev.* **2007**, *107*, 3180.
[2] Z. Li, C. Brouwer, C. He, *Chem. Rev.* **2008**, *108*, 3239.
[3] P. Pyykkö, J.-P. Desclaux, *Acc. Chem. Res.* **1979**, *12*, 276.
[4] P. Pyykkö, *Chem. Rev.* **1988**, *88*, 563.
[5] P. Schwerdtfeger, M. Dolg, W. H. E. Schwarz, G. A. Bowmaker, P. D. W. Boyd, *J. Chem. Phys.* **1989**, *91*, 1762.
[6] P. Pyykkö, *Chem. Rev.* **1997**, *97*, 597.
[7] H. Schmidbaur, *Chem. Soc. Rev.* **1995**, *24*, 391.
[8] P. Pyykkö, *Angew. Chem.* **2004**, *116*, 4512; *Angew. Chem. Int. Ed.* **2004**, *43*, 4412.
[9] S. Wang, W. Schwarz, *J. Am. Chem. Soc.* **2004**, *126*, 1266.
[10] M. Katz, K. Sakai, D. Leznoff, *Chem. Soc. Rev.* **2008**, *37*, 1884.
[11] H. Schmidbaur, A. Schier, *Chem. Soc. Rev.* **2008**, *37*, 1931.
[12] A. Vogler, H. Kunkely, *Coord. Chem. Rev.* **2001**, *219*, 489.
[13] R. Evans, P. Douglas, C. Winscom, *Coord. Chem. Rev.* **2006**, *250*, 2093.
[14] V. Yam, E. Cheng, *Top. Curr. Chem.* **2007**, *281*, 269.
[15] A. Barbieri, G. Accorsi, N. Armaroli, *Chem. Commun.* **2008**, 2185.
[16] V. Yam, E. Cheng, *Chem. Soc. Rev.* **2008**, *37*, 1806.
[17] K. Barakat, T. Cundari, M. Omary, *J. Am. Chem. Soc.* **2003**, *125*, 14228.
[18] V. Bojan, E. Fernández, A. Laguna, J. López-de Luzuriaga, M. Monge, M. Olmos, C. Silvestru, *J. Am. Chem. Soc.* **2005**, *127*, 11564.
[19] T. Lee, N. Zhu, V. Yam, *J. Am. Chem. Soc.* **2010**, *132*, 17646.
[20] R. Vogt, T. Gray, C. Crespo-Hernández, *J. Am. Chem. Soc.* **2012**, *134*, 14808.
[21] P. Schwerdtfeger, A. E. Bruce, M. R. M. Bruce, *J. Am. Chem. Soc.* **1998**, *120*, 6587.
[22] Z. Tang, A. P. Litvinchuk, H.-G. Lee, A. M. Guloy, *Inorg. Chem.* **1998**, *37*, 4752.
[23] X.-G. Xiong, P. Pyykkö, *Chem. Commun.* **2013**, *49*, 2103.
[24] M. Rawashdeh-Omary, M. Omary, H. Patterson, *J. Am. Chem. Soc.* **2000**, *122*, 10371.
[25] M. Rawashdeh-Omary, M. Omary, H. Patterson, J. Fackler, Jr., *J. Am. Chem. Soc.* **2001**, *123*, 11237.
[26] M. Iwamura, K. Nozaki, S. Takeuchi, T. Tahara, *J. Am. Chem. Soc.* **2012**, *134*, 538.
[27] M. Montalti, A. Credi, L. Prodi, M. T. Gandolfi, *Handbook of photochemistry*, Taylor and Francis, Boca Raton, **2006**.

